JOURNAL OF MATERIALS SCIENCE 7 (1972) 1099–1112

Mechanical properties of glassy carbon fibres derived from phenolic resin

K. KAWAMURA*, G. M. JENKINS
Department of Metallurgy, University College of Swansea, Swansea, UK

Mechanical properties of glassy carbon fibres produced from a phenolic resin were determined by static tensile testing. These specimens are of special interest because they consist of an isotropic core surrounded by a sheath of oriented material of varying relative thickness. The chemistry of pyrolysis of the resin is summarized and the changes in mechanical properties of the fibres are discussed in terms of the pyrolysis mechanisms. The results are compared with hardness measurements made on discs produced from the same starting material. Scanning electron microscope studies revealed that the fibres have various types of flaws both in the surface and in the core. The effect of these flaws on the fibre strength is discussed by applying Griffith crack theory.

1. Introduction

We have shown in a previous publication that glassy carbon fibres can be produced from a phenolic resin by a simple process [1]. The paper included an elementary discussion of the structure and mechanical properties of the fibres on the basis of X-ray diffraction, electron microscopy and static tensile testing. Since the previous publication was issued, the structure and mechanical properties of the fibres have been studied in more detail in addition to the detailed analysis of carbonization processes in the phenolic resin.

Detailed discussion on the formation and structure of glassy carbon is being published elsewhere [2]; this publication presents the results of mechanical property measurements made on the fibres.

2. Structure of glassy carbon and glassy fibres

The structure of glassy carbon has not been fully understood because its poor crystallinity prevents us from analysing X-ray diffraction profiles in detail and observing structural features directly with an electron microscope of low resolving power. We have recently proposed a structural model for this type of carbon after studying the pyrolysis mechanisms, and high resolution electron microscopy studies (carried out by Mr L. Ban of the Cities Service Company in America) have confirmed the structural model directly.

The structure of glassy carbon is summarized as follows: glassy carbon is made of tangled stacks of graphite-like ribbon molecules which are oriented randomly to form a network structure. The stacks of graphite-like ribbon molecules can be described as microfibrils by analogy with textile fibres and are cross-linked to adjacent microfibrils by stable carbon-carbon covalent bonds. The inter-fibrillar cross-links are strained and so are less thermally stable than the graphitic trigonal bond within ribbons. They are thus progressively ruptured at high temperatures, which is responsible for visco-elastic behaviour about 2500°C. The scission of inter-fibrillar cross-link bonds results in an increase in "defect distance" or the average relatively strain-free length of the microfibril, and a decrease in inter-layer spacing of graphitic ribbon molecules which are stacked uniformly above each other to form a microfibril.

Carbon fibres made from phenolic resin have similar crystallographic parameters to those of bulk glassy carbon. No appreciable preferred orientation can be detected easily in carbonized fibres heat-treated below 2000°C. However, scanning electron microscopy, electron diffraction and polarized light microscopy studies confirm that the surface of the carbonized fibres is textured, in that the ribbons are stretched along

*Now at Nihon University, Tokyo, Japan.

the fibre axis and are stacked radially; the thickness of the textured sheath increases at the expense of the isotropic core with heat-treatment.

Therefore, the carbonized fibres have a double structure: an isotropic core surrounded by an anisotropic textured sheath, the structure of which is very similar to that of well-oriented carbon fibres in that it does not give rise to any bands other than (000*l*) and (*hk**0) in an X-ray diffraction pattern. Moreover, scanning electron microscope studies indicate that the surface orientation in the carbonized fibres is a reproduction of molecular orientation induced in the surface of the polymer fibre during the melt-extrusion process. Thus surface orientation in the carbonized fibre is responsible for a gradual increase of the tensile modulus with decrease of fibre diameter, as suggested previously.

The surface orientation is not an example of the two-phase graphitization which is observed in many non-graphitizing carbons. A clear-cut boundary is not observed between the isotropic core and the anisotropic sheath, indicating that the degree of the orientation decreases gradually from the surface to the core along the radial direction. Fig. 1 shows a polarized light micrograph of cross-sections of the fibres heat-treated at 2500°C, which confirms this.

In another paper [2] we give evidence to show that orientation in the outer sheath is effected by air-oxidation to form stable cross-links or nodes between stretched polymer chains immediately after extrusion. These are remembered even after chain-retraction resulting from thermal agitation on heating through the carbonization cycle. On heating above 2500°C, the ribbons derived from the coalescence of neighbouring chains straighten out and begin to pull against well established nodes in the network. In the core these will allow a random arrangement. In the sheath their spatial arrangement reflects the pattern set in by oxidation of the original oriented polymer chain.

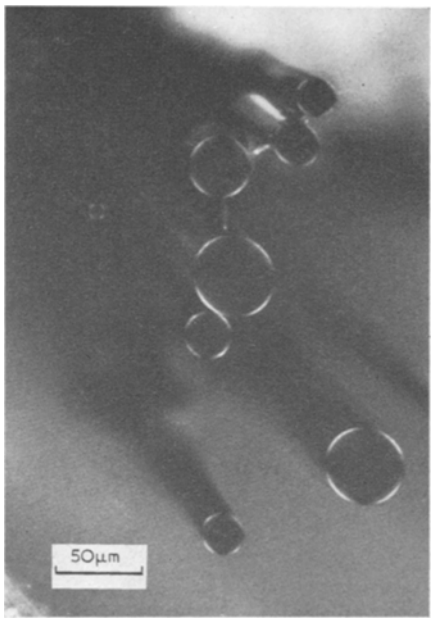

Figure 1 Polarized light micrograph of fibre cross-section annealed at 2500°C.

3. Summary of carbonization mechanisms

X-ray diffraction, infra-red spectroscopy, chemical analysis and physical property measurements such as volume shrinkage, density and electrical resistivity indicate that the phenolic resin goes through the following distinct stages of carbonization:

(1) The initial phenolformaldehyde-type polymer chains coalesce to form imperfect aromatic ribbon molecules which are clustered together in fibrils with elimination of water. The formation of ribbon molecules starts at a heat-treatment temperature of 350°C. (2) A rapid increase in volume shrinkage takes place as a function of hydrogen-carbon ratio at 700°C, indicating that the fibrils start approaching each other to form inter-fibrillar cross-link bonds with elimination of hydrogen. This process is accompanied by a steep decrease in electrical resistivity. The formation of inter-fibrillar cross-link bonds prevents further rearrangement of ribbon molecules, resulting in almost constant crystallographic parameters between 1000 and 1500°C. (3) Above 1500°C, a gradual annealing takes place. The inter-layer spacing decreases and the apparent crystallite sizes increase with heat treatment, implying that the ribbons are gradually achieving degrees of straightness and parallelism by rupture and reformation of inter-fibrillar bonds. The final structure (above 2500°C), comprising a network of stacked graphitic ribbons, achieves as much perfection as possible within the restrictions imposed by the presence of strong nodes in the ribbon network and the finite width of the ribbons. Fig. 2 shows a high resolution electron micrograph of the phenolhexamine-based glassy carbon heat-treated at 2700°C, which reveals the structural features of glassy carbon at this annealing stage.

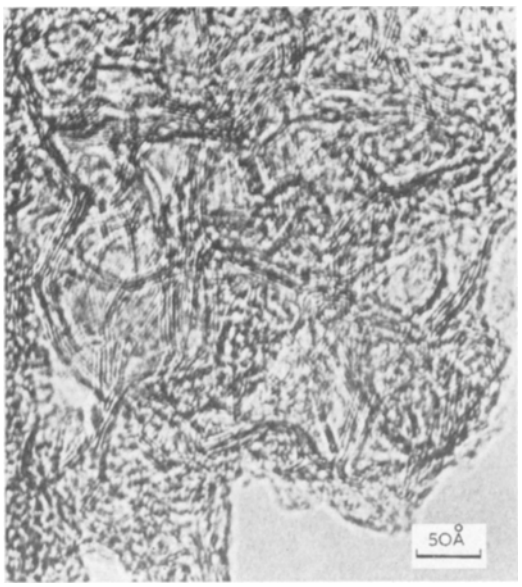

Figure 2 High resolution electron micrograph of glassy carbon annealed at 2700°C.

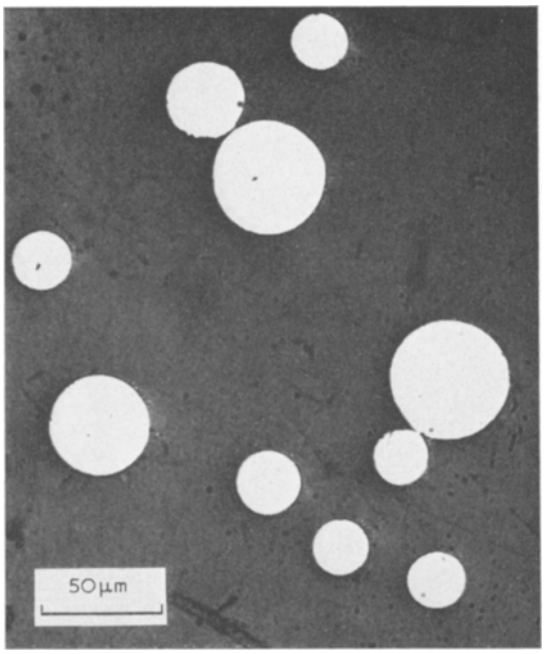

Figure 3 Typical fibre cross-sections showing cylindrical perfection at all possible diameters.

4. Mechanical properties of glassy carbon fibres

4.1. Experimental procedures

The most critical factor in determining mechanical properties of the fibres by static tensile testing was measurement of the diameter. If cross-sections of fibres had irregular shapes, the determination of cross-section area would be very difficult. However, our fibres had reasonably circular cross-sections as shown in Fig. 3. The diameter was determined with a Vickers optical microscope, calibrated using various commercial carbon fibres, the diameter of which had been determined by the manufacturers.

Tensile testing was carried out using an Instron tensile testing machine. A load cell, the minimum load range of which is 0 to 10 g, was employed. A load cell deflection of 2.5 μm/g up to a load of 10 g was taken into account in determining fracture elongation and tensile modulus. Our fibres had relatively low Young's moduli and therefore the load cell deflection was much less significant than for commercial high-modulus carbon fibres.

Both ends of a fibre sample were fixed to a cardboard frame using an epoxy resin (Araldite). Both sides of the cardboard frame were cut with a pair of scissors before the sample was pulled. A gauge length of 1 cm was generally chosen. However, fracture elongation decreased with heat-treatment above 1000°C and the fibres heat-treated above 1500°C showed very small fracture elongation. For these samples, a gauge length of 2 cm was also examined. The sample was pulled at a strain-rate of 0.005 cm/min.

4.2. Elasticity and hardness

Fig. 4 shows the variation of Young's modulus of the fibre as a function of heat-treatment temperature. The modulus increases by 20% after heat-treatment at 350°C. This corresponds to the formation of intermolecular cross-links between phenolformaldehyde-type chain-molecules. The intermolecular cross-links result from the reaction between hydroxyl groups in phenolic linkages in one polymer chain and methylene bridges connecting phenolic groups in a neighbouring chain, with elimination of water.

The modulus remains constant at heat-treatment temperatures between 350 and 500°C. At this carbonization stage, the cross-linked polymer is modified into an open network of long, narrow and imperfect aromatic ribbon molecules. The scission of aliphatic ether linkages ($-CH_2-O-CH_2$) which have been detected as a minor constituent of the original chain molecules, increases the mobility of the polymer chains and so accelerates their coalescence. This results in an increase in

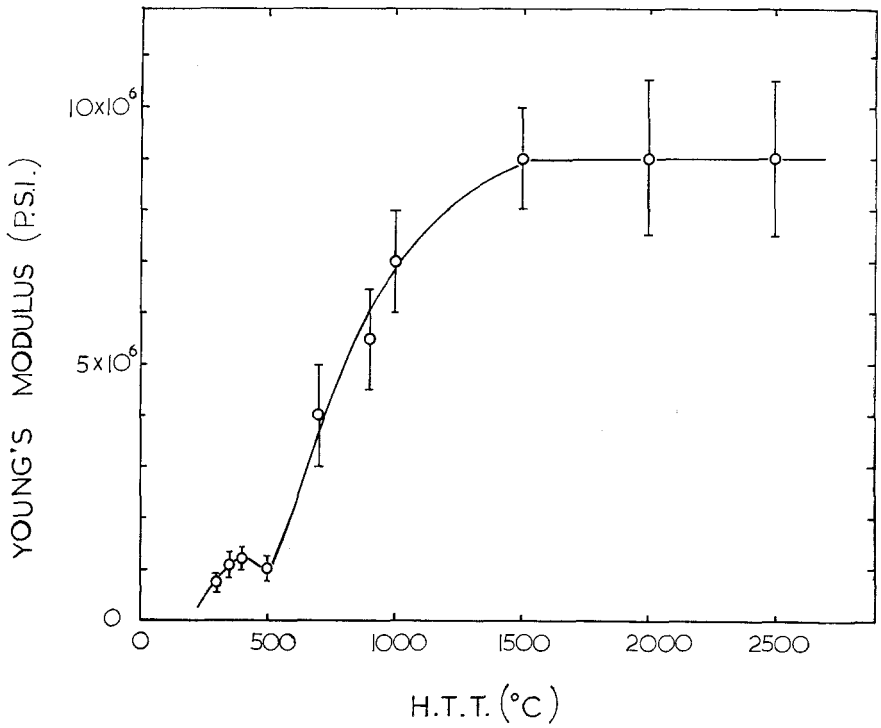

Figure 4 Variation of Young's modulus of fibre as a function of heat-treatment temperature.

length of the ribbon molecules, but it does not increase the modulus because of the chain scission and the large gaps left by the elimination of water molecules from the original network. The ribbon molecules tend to be clustered together to form incipient microfibrils.

Above 500°C, the modulus increases rapidly with heat-treatment and reaches a constant value at 1500°C. This is due to the formation of inter-fibrillar cross-link bonds between the microfibrils or clustered ribbon molecules, with elimination of hydrogen.

The modulus is almost constant for heat-treatment temperatures between 1500 and 2500°C. Since interlayer spacing decreases and apparent crystallite size increases in this heat-treatment region, some of the inter-fibrillar cross-link bonds are considered to be ruptured, which should result in a decrease in the modulus. The constant value of the modulus is due to the double structure of the fibres as discussed below in detail.

It is interesting to compare the results of modulus measurements on fibres with hardness measurements made on glassy carbon discs prepared from the same phenolic resin. Fig. 5 shows the variation of the Vickers hardness of the glassy carbon disc as a function of heat-treatment temperature. The hardness shows a similar behaviour to that of the modulus up to a heat-treatment temperature of 1500°C, but it decreases considerably at higher heat-treatment temperatures.

Fig. 6 illustrates the relationship between the hardness of *discs* and the tensile modulus of *fibres* up to a firing temperature of 1500°C, indicating that the tensile modulus of the fibres is approximately proportional to the hardness of the discs. The increase in the hardness and the modulus with heat-treatment between 500 and 1500°C suggests that intermolecular forces between fibrils are increased by the formation of inter-fibrillar cross-links. The ribbon molecules in a fibril contain foreign atoms, mainly hydrogen, in the periphery and therefore the formation of the cross-link bonds should accompany elimination of hydrogen. Fig. 7 shows the variation of the hardness as a function of hydrogen-carbon atomic ratio, suggesting that elimination of hydrogen from the periphery of a ribbon molecule leads to the formation of inter-fibrillar cross-link bonds. This results in an

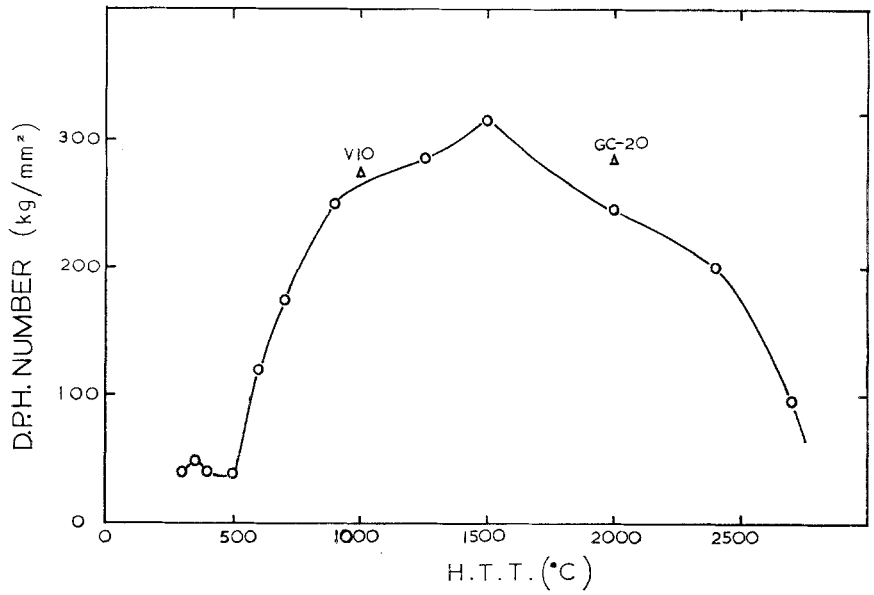

Figure 5 Variation of Vickers hardness of glassy carbon discs as a function of heat-treatment temperature.

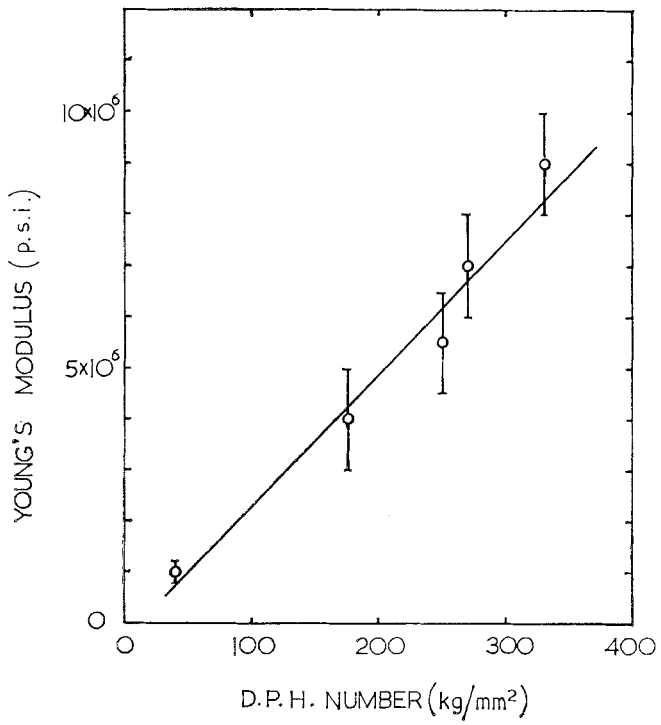

Figure 6 Relationship between Vickers hardness of discs and tensile modulus of fibres at various firing temperatures up to 1500°C.

appreciable dimensional shrinkage and a marked decrease in electrical resistivity, but it does not promote much crystallographic change because the formation of stable covalent cross-links prevents further release of internal strain energy in ribbon molecules and, therefore, also prevents their lateral growth from mutual coalescence.

Provided that the fibre has the same crystallographic structure as the bulk sample, then on the basis of disc hardness data the elastic

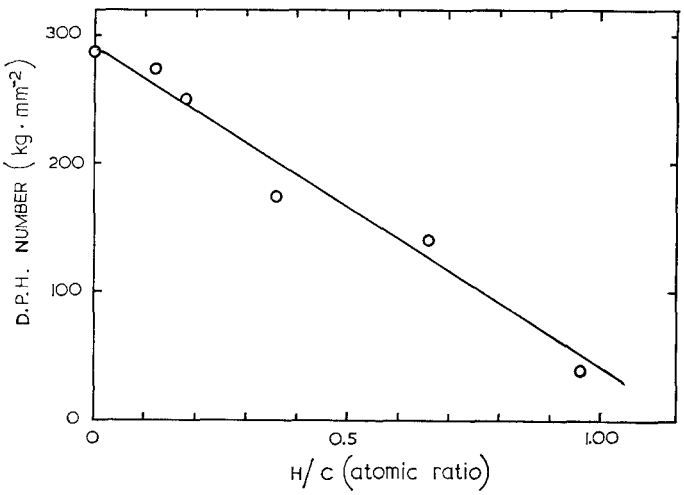

Figure 7 Variation of hardness as a function of hydrogen-carbon atomic ratio.

modulus of the fibre would have been expected to decrease above 1500°C, but in fact it does not. This discrepancy can be explained in terms of the double structure of the fibres. The carbonized fibre has an anisotropic textured sheath surrounding an isotropic core. The thickness of the textured sheath increases with heat-treatment temperature and it can be detected by polarized light micrography after heat-treatment above 1500°C. Since Young's modulus of carbon is very sensitive to the preferred orientation of carbon layers, the tensile modulus of the fibre is a critical function of the relative thickness of the textured sheath.

Above 1500°C, the tensile modulus of the isotropic core in the fibre should decrease with increase in heat-treatment temperature because the hardness of the isotropic glassy carbon disc decreases. However, the thickness of the textured sheath increases with heat-treatment temperature, which compensates for a decrease in the tensile modulus of the core. This is responsible for the constant value of the modulus above 1500°C.

4.3. Tensile strength

Fig. 8 shows the variation of ultimate tensile strength of relatively thick fibres of diameter 25 μm as a function of heat-treatment temperature. The average tensile strength increases rapidly with heat-treatment temperature up to 1000°C and thereafter decreases gradually. The sharp increase in the tensile strength corresponds to an increase in the tensile modulus and hardness in the same temperature region. This suggests that the increase in the intermolecular cohesion between fibrils also results in an increase in the tensile strength. Fig. 9 illustrates the relationship between the ultimate tensile strength and the hardness, showing that the harder material is also stronger.

It is important to note that the ultimate tensile strength of the fibre is considerably higher than that of commercial bulk glassy carbon. Moreover, the fibre strength increases with decrease of fibre diameter, as reported previously. These properties are very similar to those observed in glass and glass fibres.

Fig. 10 shows the variation of the fibre strength as a function of the reciprocal of fibre diameter. This indicates that the fibre strength is proportional to the reciprocal of fibre diameter, as expressed by the following empirical formula:

$$\sigma = \sigma_\infty + Kd^{-1} \qquad (1)$$

where σ is the fibre strength, d is the fibre diameter and σ_∞, K are constants. σ_∞ and K are estimated to be 24000 psi (168 MNm^{-2}) and 430 pound in^{-1} (11 MNm^{-1}). The empirical formula is very similar to that proposed by Griffith [3] for glass fibres.

It is considered that σ_∞ (which corresponds to $d = \infty$) represents the tensile strength of bulk glassy carbon. It is somewhat higher than that actually observed, the highest tensile strength obtained so far being 15000 psi (105 MNm^{-2}) [4]. This discrepancy is likely to be due to the

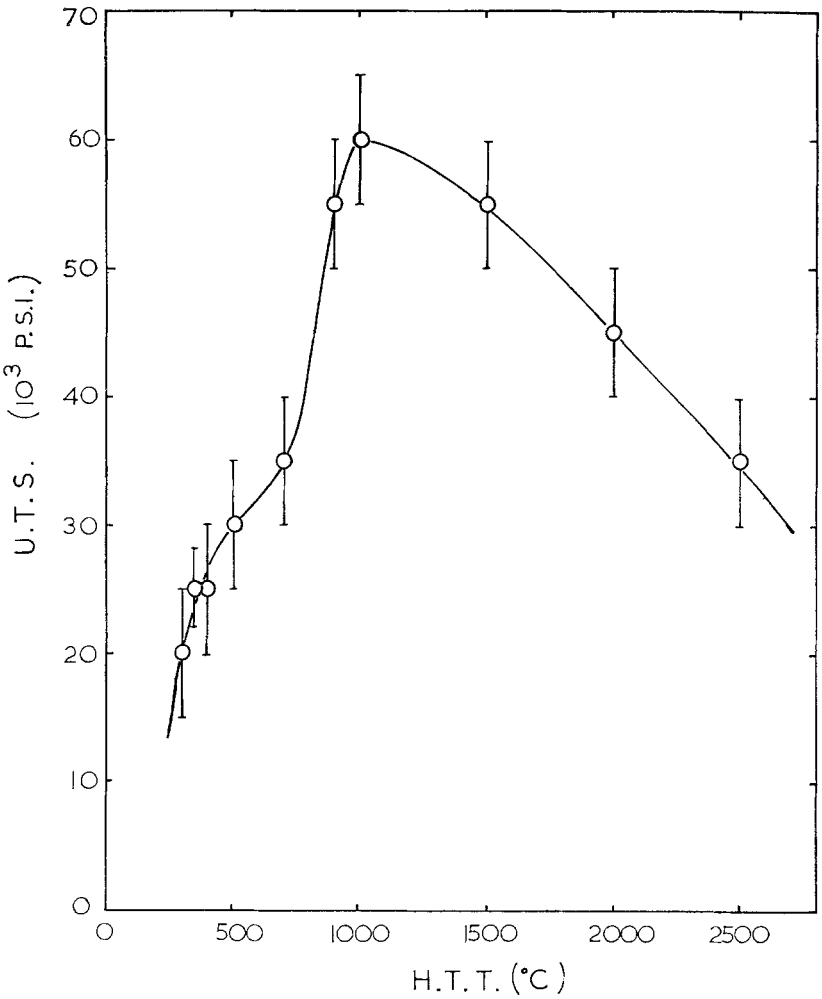

Figure 8 Variation of ultimate tensile strength of thick fibres as a function of heat-treatment temperature.

difficulty of machining glassy carbon without causing serious damage to the surface.

Fig. 11 shows the variation of the reciprocal of the tensile strength as a function of fibre diameter. A more appropriate empirical formula would then be:

$$\frac{1}{\sigma - \sigma_\infty} = \frac{1}{\sigma_0 - \sigma_\infty} + \frac{d}{K} \qquad (2)$$

where σ_0 would be the ultimate tensile strength of an infinitely thin fibre. From this diagram, it is possible to estimate the ultimate strength of glassy carbon fibres as d approaches zero to be about 400×10^3 psi (2.8 GNm^{-2}). The Young's modulus of bulk material is usually taken to be 4×10^6 psi (28 GNm^{-2}) (see Fitzer and Schaffer [4]). It is, therefore, possible that the ultimate theoretical strength of glassy carbon can be achieved in very thin fibre.

It is important, however, to note that the ultimate strength (σ_0) estimated above is not the strength of isotropic material because of the increase in the thickness of the textured sheath relative to fibre diameter as the diameter decreases, (which, as reported previously [1], causes the Young's modulus to increase with decrease in fibre diameter). Accordingly, the theoretical strength of the fibre (if taken to be a fixed fraction of the Young's modulus) should be higher than that estimated. This indicates that the fibres have microscopic points of weakness which are independent of the orientation of individual microfibrils and cannot be eliminated by aligning the fibrils along the fibre axis. In fact,

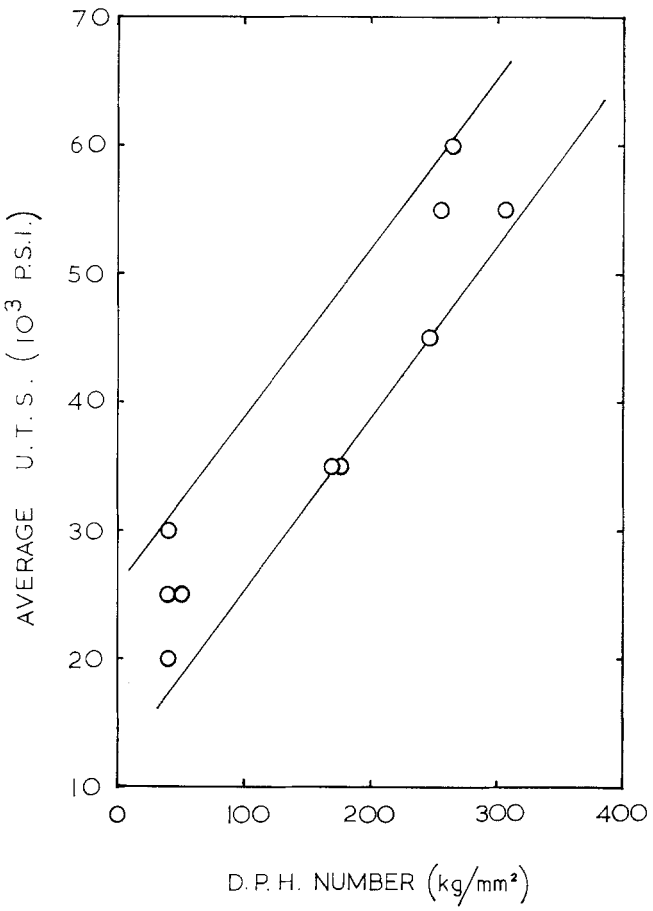

Figure 9 Relationship between ultimate tensile strength (fibres) and hardness (discs).

Hawthorne [6] has shown that glassy carbon fibres have a high degree of preferred orientation and high tensile modulus, after hot-stretching, but the tensile strength is much lower than the theoretical strength estimated from the modulus.

The marked increase in tensile strength with decrease in the fibre diameter suggests that the fibres have various macroscopic flaws, the size and concentration of which are dependent on the fibre diameter. These flaws are observed in commercial carbon fibres [7, 8].

5. Observation of flaws in the fibres

Direct observations of carbonized and fractured surfaces of the fibres were made using a scanning electron microscope. The samples were coated with a thin gold film before examination.

The results reveal that both polymer and carbon fibres have various flaws both in the surface and in the core. Fig. 12 shows representative surface flaws in the fibres. Fig. 12a reveals surface flaws elongated along the fibre axis in a fibre heat-treated at 300° C. This type of flaw is created during the melt extrusion process which stretches and elongates spherical voids along the fibre axis. Fig. 12b shows a much smaller surface void in a fibre heat-treated at 1500° C, probably formed by the escape of volatile products through the surface during carbonization. Fig. 12c shows minute surface "stretch" cracks in the fibre heat-treated at 500° C, formed mechanically during pyrolysis because the fibres are slightly restrained on a porous asbestos tray up to a heat-treatment temperature of 400° C.

Fig. 13 shows the presence of internal flaws in both polymer and carbon fibres, as-spun (Fig. 13a) and after heat-treatment to 1500 and 2500° C (Figs. 13b and c respectively). It is considered that these flaws are created during polymerization and carbonization by similar mechanisms to

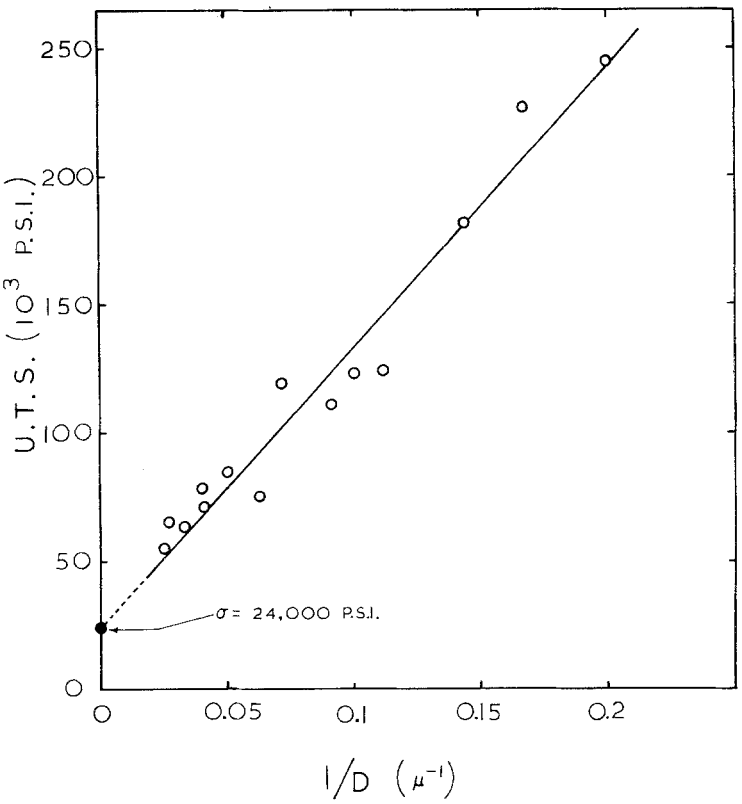

Figure 10 Fibre strength as a function of the reciprocal of fibre diameter. (Heat-treatment temperature 900° C.)

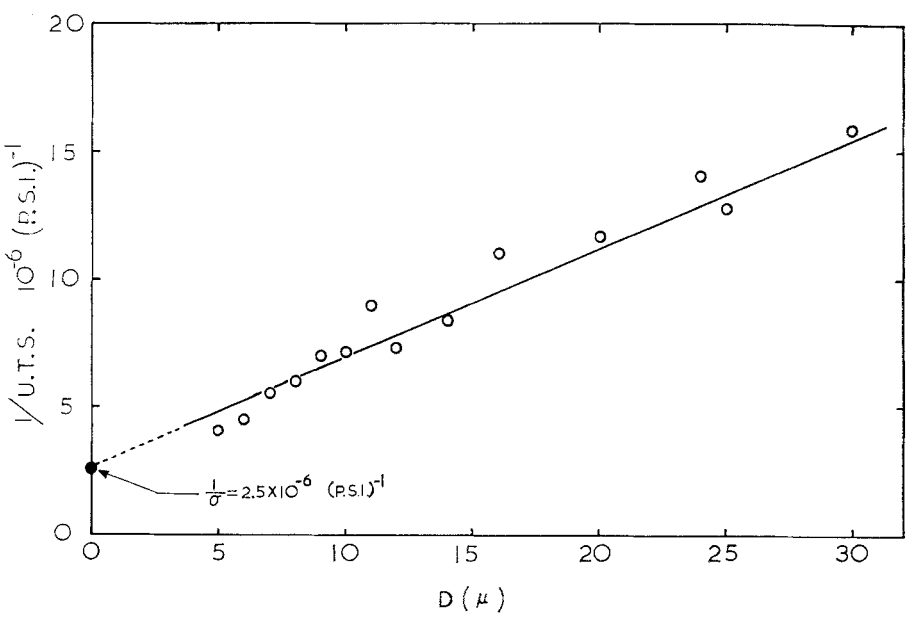

Figure 11 Reciprocal of the tensile strength as a function of fibre diameter. (Heat-treatment temperature 900° C.)

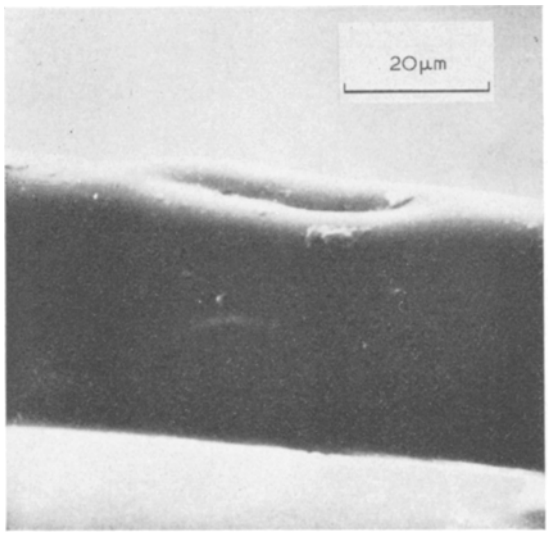

(a)

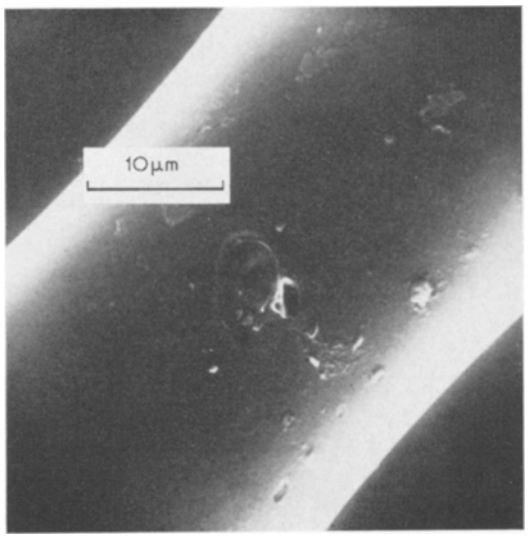

(b)

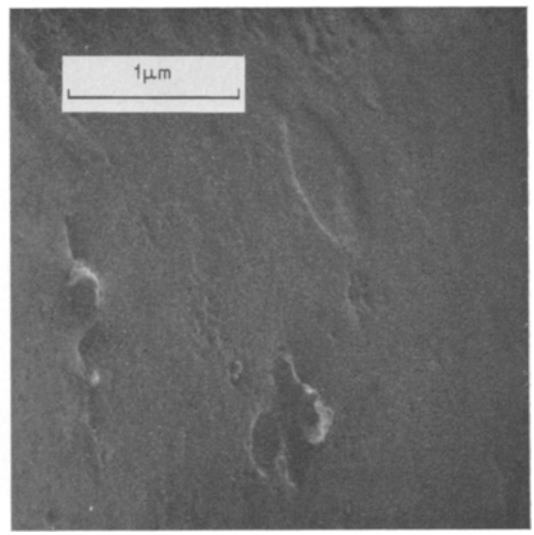

(c)

Figure 12 (a) Surface flaw elongated along fibre axis (HTT 300°C). (b) Typical surface void (HTT 1500°C). (c) Minute surface cracks formed mechanically (HTT 500°C).

those producing the surface voids shown in Figs. 12a and b.

6. A discussion on the elastic behaviour

The Young's modulus of the thicker carbon fibres is about twice as high as that of commercial bulk glassy carbon for the same heat-treatment temperature [5]. Bacon and Smith [9] have obtained a similar result with cellulose-based carbon fibres. They claim that the initial preferred orientation in cellulose fibres remains to some extent in the high-temperature annealed fibres. At intermediate heat-treatment temperatures (below 2000°C) the preferred orientation is not discernible.

The present evidence can be explained in terms of the "memorized" surface orientation in the carbon fibres, in that the molecular orientation induced in the surface of the polymer fibres during the melt-extrusion process is "memorized" during pyrolysis, and therefore the surface of the fibres carbonized even at low temperatures is more textured than the core.

Above 1500°C heat-treatment temperature, the surface orientation is clearly observed with a polarized light microscope. For these fibres, the tensile modulus is approximately written as:

$$E = f_1 E_1 + (1 - f_1) E_2 \qquad (3)$$

where E is the tensile modulus of the composite fibre, E_1, E_2 are the tensile moduli of the anisotropic sheath and the isotropic core respectively, and f_1 is the fraction of cross-sectional area of anisotropic sheath. Putting α for the ratio of the thickness of the textured sheath to the radius of the isotropic core, Equation 3 is written as:

$$E = \frac{\alpha(\alpha + 2)}{(\alpha + 1)^2} E_1 + \frac{1}{(\alpha + 1)^2} E_2 \qquad (4)$$

It is possible to estimate the thickness of the

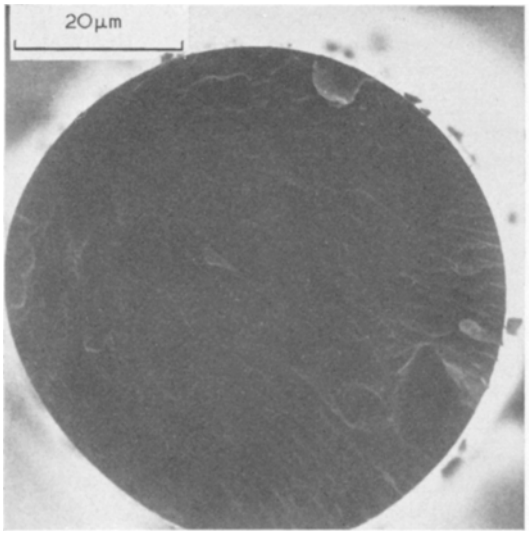

(a)

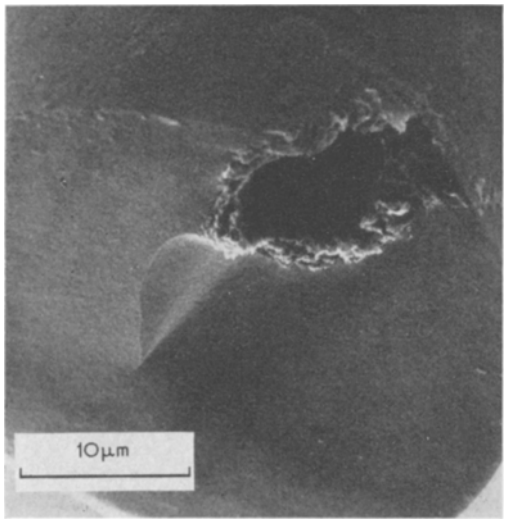

(b)

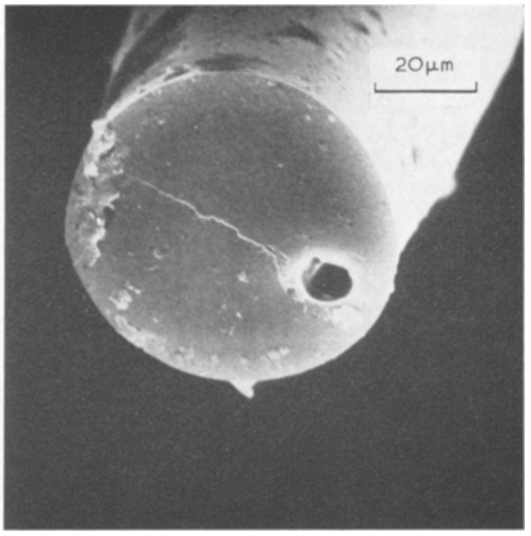

(c)

Figure 13 (a) Large internal flaw (as spun fibre). (b) Large internal flaw (HTT 1500°C). (c) Large internal flaw (HTT 2500°C).

textured sheath and the ratio (α) from Fig. 1. For instance, fibre with a diameter of 50 μm has a textured sheath of thickness about 2.5 μm and, therefore, α is about 0.05. Assuming that the modulus of the isotropic core is proportional to the hardness of isotropic bulk glassy carbon, the core modulus is estimated to be about 3×10^6 psi (21 GNm^{-2}) after heat-treatment to 2500°C. The following relation, based on Fig. 6, is used:

$$E\,(\text{HTT } 2500^\circ\text{C}) = \frac{\text{DPH (HTT } 2500^\circ\text{C)}}{\text{DPH (HTT } 1000^\circ\text{C)}} \times E\,(\text{HTT } 1000^\circ\text{C})$$

Since the structure of the textured sheath is very similar to that of well oriented carbon fibres, the tensile modulus of the sheath should be comparable to that of highly textured carbon fibres, in which case E_1 should be about 60×10^6 psi (420 GNm^{-2}). The overall tensile modulus calculated for the fibres of Fig. 1, using Equation 4 is about 8×10^6 psi (56 GNm^{-2}), which agrees well with that observed.

Otani [10] observed that the tensile modulus of isotropic carbon fibres from polyvinyl chloride pitch also increases with decrease of fibre diameter; it is inferred that these fibres have similar structural features to those of our glassy carbon fibres.

In general, Young's modulus, as well as hardness, of glassy carbon is very high for an isotropic "non-crystalline" carbon. This is due to the presence of the stable inter-fibrillar cross-links which prevent aromatic ribbon molecules in the fibrils from shearing past each other. The nature of the inter-fibrillar cross-links is not fully understood. High temperature visco-elastic properties of glassy carbon are more pertinent to the elucidation of this problem.

Ruland [11] proposes a new model for the

elastic response of carbon fibres, termed "elastic unwrinkling", in which he assumes that the component ribbons are bent by mutual cohesion at nodes. A stress on these ribbons will increase the preferred orientation. The environment of the ribbons resists the tilting of the layers and a component of the stress causes an elongation of the ribbons. He proposes that the axial Young's modulus of the fibres (E_c) is to be given by

$$\frac{1}{E_c} = l_z S_{11} + m_z S^*$$

S_{11} is the elastic compliance of a graphite sheet in the plane of the sheet and S^* is the "environmental" compliance related to the ease of "dewrinkling" the ribbons with respect to their "environment" (boundary restraint):

$$l_z = \frac{\int_0^{\pi/2} \cos^2(\phi)\, g(\phi)\, d\phi}{\int_0^{\pi/2} \sin\phi\, g(\phi)\, d\phi}$$

$$m_z = \frac{\int_0^{\pi/2} \sin^2(\phi)\, g(\phi)\, d\phi}{\int_0^{\pi/2} \sin\phi\, g(\phi)\, d\phi}$$

where $g(\phi)$ is the distribution of layer normals as determined by X-ray scattering techniques.

l_z approaches 1 and m_z approaches 0, for perfect alignment of ribbons along the fibre axis.

$$S_{11} = 0.985 \times 10^{-12}\ \mathrm{m^2N^{-1}}$$
$$S^* = 27.5 \times 10^{-12}\ \mathrm{m^2N^{-1}}$$

For isotropic fibres, $l_z = m_z = \pi/4$, whence E_c is predicted to be 4.5×10^6 psi (31.5 $\mathrm{GNm^{-2}}$), very close to that measured here for thick fibres.

As the heat-treatment temperature increases above 1000°C, the environmental restraint decreases and so S^* increases. Graphite ribbons produced at low temperatures must contain a large population of grown-in defects. These cause small dimples or wrinkles in the ribbons which effectively lower the stiffness of the sheet in an a-axis direction so that S_{11} is effectively larger than that for a perfect sheet. When the ribbons are annealed at graphitizing temperatures and pulled taut between strong nodes in the ribbon network, the out-of-plane defects are progressively removed by a process such as vacancy climb and the effective S_{11} is reduced to that of a perfect sheet.

Thus the Young's modulus of isotropic fibres should be rather low, because, for them, S^* is predominant. For anisotropic fibres the modulus should increase because S_{11} is then predominant. In our two-phase fibres the modulus remains constant above 1000°C – the effect of a compromise.

6.1. A discussion on strength and fracture mechanics

The strength of the glassy carbon fibres is considered to be sensitive to flaws or defects observed both in the surface and in the core. It must also be related to intermolecular forces between fibrils and structural features within fibrils.

The first factor is highly dependent on the pyrolysis process and preparation techniques and is not an intrinsic property of the fibres, while the latter factors are intrinsic to the structure of the material. Scanning electron microscopy shows that fracture of the fibres is almost exclusively associated with surface or internal flaws.

The Griffith crack theory predicts that the critical fracture stress normal to the plane in which fracture takes place is given by

$$\sigma^2 = \frac{2EU}{\pi C} \qquad (5)$$

where E is the Young's modulus governing the interaction of atom planes in a direction normal to the fracture plane, U is the surface energy released per unit area exposed by the propagation of the crack and C is the length of the crack.

It is possible to estimate the length of the cracks in the fibres from the experimental results shown in Figs. 4 and 8. According to Good *et al* [12], the surface energy for the basal plane in graphite is 0.1 $\mathrm{Jm^{-2}}$. If this value is assumed in a typical fibre with $E = 60$ $\mathrm{GNm^{-2}}$ and $\sigma = 2$ $\mathrm{GNm^{-2}}$, the critical crack length is calculated to be about 10^{-7} cm. On the other hand, the surface energy in well oriented fibre is estimated elsewhere [13] to be 4.2 $\mathrm{Jm^{-2}}$. Using this value, the critical crack length becomes 4.10^{-6} cm. Even this revised estimate is much smaller than the diameters of the typical large internal flaws shown in Fig. 12.

It is concluded that microcracks, rather than large internal flaws, are the prime initiators of fracture. Fig. 14 illustrates this point with a stereoscan image of a typical failure initiated at a surface microcrack in a fibre annealed at 900°C. However, fracture is associated in many cases

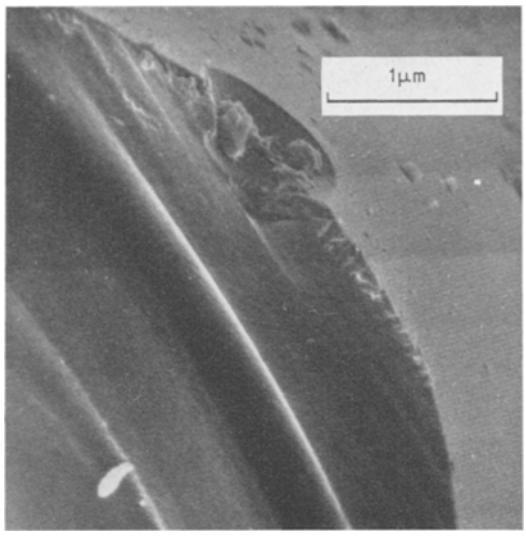

Figure 14 Typical fracture at surface microcrack (fibre annealed at 900°C).

with the large internal flaws such as can be seen in Fig. 13. It may be that microcracks are associated with both the outer surface of the fibre and the surface of the large internal flaws as proposed by Sharp and Burnay [8].

The effect of fibre diameter on the strength indicates that the thinner fibre has a lower concentration of critical flaws. In other words, the average size of flaws decreases with decrease of fibre diameter. It is deduced from Equations 1 and 5 that the average length of the critical crack is proportional to the square of the fibre diameter or to the cross-sectional area of the fibre. It is difficult, however, to analyse this relationship theoretically because the flaws in the fibres are formed by different processes, both mechanical and chemical. During pyrolysis, the polymer liberates various volatile products, accompanied by a large dimensional shrinkage. The internal pressure, built up by these gases before they can escape to the surface by diffusion, prevents molecular retraction and coalescence and, therefore, results in the formation of flaws.

It is reasonable to assume that the concentration of internal flaws is higher in thick carbon fibres than in thin carbon fibre, because the thinner fibre has the larger ratio of free surface area to volume, which makes gas escape easier through the surface during pyrolysis. Moreover, the surface of the thinner fibre can stand the higher internal gas pressure due to volatile products because of increased surface tension. This results in a lower concentration of surface flaws in the thinner carbon fibre. Therefore, the thinner carbon fibre has the lower concentration of both internal and surface flaws, which qualitatively explains the increase of the tensile strength with decrease of fibre diameter. This consideration is consistent with the fact that thick glassy carbon artefacts cannot be prepared generally without producing pores and cracks on a macroscopic scale.

It is not easy to explain the decrease in the average tensile strength of the fibres with heat-treatment above 1000°C. Provided that the fibres do not contain any inorganic or metallic impurities, it is unlikely that extra critical flaws are created in the fibres at heat-treatment temperatures above 1000°C. Therefore, the decrease in strength should be due to a change of intrinsic structural features in the fibres.

As described previously, a gradual annealing takes place above 1500°C and the ribbon molecules in the fibrils gradually straighten and become parallel with the rupture and reformation of inter-fibrillar bonds, accelerating the release of strain energy in the fibrils. Annealing increases the average relatively strain-free length of the fibrils, as shown by the increase in the apparent crystallite diameter L_a. This could make crack propagation easier along the basal plane of the ribbon molecule in the fibrils.

On the other hand, the thickness of the textured sheath increases with heat-treatment above 1000°C in our fibrils. Therefore, the periphery of the isotropic core is progressively textured, suggesting that the original network of tangled and twisted fibrils is changed to a network of elongated and parallel fibrils without any appreciable elongation in fibre length. Some of the tangled fibrils must be broken into shorter and relatively straightened fibrils by way of accommodation, producing further points of weakness in the fibres. In order to avoid this, the tangled fibrils should be elongated gradually under tension, by stretching the fibres during heat-treatment.

Of course, part of the fibre is oriented while part is not. Thus more general internal strains will be induced because of differences in thermal expansion coefficients. Again, a slower heating and cooling cycle with a long holding time above 2000°C should remove much of the strain. It is tempting to speculate whether commercial polyacrylonitrile carbon fibres are also composite fibres (with an isotropic core surrounded by

a relatively thicker sheath than for phenolic resin fibre) since they also show similar effects.

Acknowledgement

We are indebted to the National Coal Board for the sponsorship of this research, to Mr L. L. Ban of Cities Services Company in America, for carrying out high resolution electron microscopy studies and to Mr F. Rutter of the British Steel Corporation for his kind help in taking the polarized light micrographs.

References

1. K. KAWAMURA and G. M. JENKINS, *J. Mater. Sci.* **5** (1970) 262.
2. G. M. JENKINS, K. KAWAMURA, and L. L. BAN, *Proc. Roy. Soc.* A **327** (1972) 501.
3. S. S. GRIFFITH, *Phil. Trans. Roy. Soc.* A **221** (1920) 163.
4. E. FITZER and W. SCHAFFER, *Carbon* **8** (1970) 353.
5. R. E. TAYLOR and D. E. KLINE, *ibid* **5** (1967) 607.
6. H. M. HAWTHORNE, "The International Carbon Fibres Conference" (Plastics Institute, London, 1971).
7. J. W. JOHNSON and J. D. THORNE, *Carbon* 7 (1969) 659.
8. J. V. SHARP and S. G. BURNAY, "The International Carbon Fibres Conference" (Plastics Institute, London, 1971).
9. R. BACON and W. H. SMITH, "The Second Conference on Industrial Carbon and Graphite" (Soc. Chem. Ind., London, 1965).
10. S. OTANI, *Carbon* **3** (1965) 31.
11. W. RULAND, "The International Carbon Fibres Conference" (Plastics Institute, London, 1971).
12. R. J. GOOD, L. S. GIRIFALCO, and G. J. KRAUS, *J. Phys. Chem.* **62** (1958) 1418.
13. W. N. REYNOLDS, "The Third Conference on Industrial Carbon and Graphite" (Soc. Chem. Ind., London, 1970).

Received 24 September 1971 and accepted 18 April 1972.